European Journal of Mechanics A/Solids 45 (2014) 143–152

Contents lists available at ScienceDirect

European Journal of Mechanics A/Solids

journal homepage: www.elsevier.com/locate/ejmsol

Nonlinear vibration analysis of Timoshenko nanobeams based on surface stress elasticity theory

R. Ansari*, V. Mohammadi, M. Faghih Shojaei, R. Gholami, H. Rouhi

Department of Mechanical Engineering, University of Guilan, P.O. Box 41635-3756, Rasht, Iran

A R T I C L E   I N F O

Article history:
Received 21 May 2013
Accepted 4 November 2013
Available online 3 December 2013

Keywords:
Nanobeam
Nonlinear free vibration
Surface stress elasticity

A B S T R A C T

In this article, the nonlinear free vibration behavior of Timoshenko nanobeams subject to different types of end conditions is investigated. The Gurtin–Murdoch continuum elasticity is incorporated into the Timoshenko beam theory in order to capture surface stress effects. The nonlinear governing equations and corresponding boundary conditions are derived using Hamilton's principle. A numerical approach is used to solve the problem in which the generalized differential quadrature method is applied to discretize the governing equations and boundary conditions. Then, a Galerkin-based method is numerically employed with the aim of reducing the set of partial differential governing equations into a set of time-dependent ordinary differential equations. Discretization on time domain is also done via periodic time differential operators that are defined on the basis of the derivatives of a periodic base function. The resulting nonlinear algebraic parameterized equations are finally solved by means of the pseudo arc-length continuation algorithm through treating the time period as a parameter. Numerical results are given to study the geometrical and surface properties on the nonlinear free vibration of nanobeams.

1. Introduction

During the last decade, many studies have been carried out on the behavior and applications of nanobeams. They can be used in nano-irradiation (Kirkby et al., 2007), fluctuation electron microscopy (Daulton et al., 2010), strain sensors (Hu et al., 2010) and optical nanocavities (Maksymov, 2011; Shambat et al., 2011). The mechanical characteristics of nanobeams such as bending, buckling and vibration are increasingly gaining interest in nanomechanics due to their significance for nanobeam-based devices. Because of high surface to bulk ratio, nanobeams behave in a different way from beams at macroscale. Surface stress is one of the most important effects which leads to unusual mechanical behavior of these nanostructures. For example, according to atomic force microscope (AFM)-based bending tests on chromium nanobeams (Nilsson et al., 2003, 2004), it was revealed that the nanobeam response is considerably affected by surface residual stress. This effect can be explained by the fact that atoms at or near a free surface of nanobeam have various equilibrium requirements in comparison with atoms within the bulk of material due to different environmental conditions. Many researchers have investigated the surface stress effect on the behavior of different nanostructures such as nanocavities, nanoplates, nanobeams and nanowires (e.g., see (Dingreville et al., 2005; Li et al., 2006; Wang et al., 2010; Miri et al., 2011; Ansari and Sahmani, 2011a; Sadeghian et al., 2011; Assadi, 2012; Liu et al., 2012; Narendar et al., 2012; Narendar and Gopalakrishnan, 2012; Elishakoff et al., 2012)). Among different theoretical approaches, the surface stress elasticity theory proposed by Gurtin and Murdoch (1975, 1978)) has been widely applied to study the surface stress effect on the mechanics of nanobeams. Herein, some of the relevant published papers on the surface stress models of nanobeams are cited.

Based on the Gurtin and Murdoch's elasticity and Euler-Bernoulli beam theory, Fu et al. (2010) studied the free vibration and buckling of nanobeams in both linear and nonlinear regimes. They used the Galerkin method to develop a reduced-order model and applied the incremental harmonic balanced method to investigate the amplitude-frequency response of nanobeams. Bar On et al. (2010) developed a continuum model for nanobeams, including both surface stress effects and material heterogeneity and compared it with atomistic simulations. They found that the continuum model needs a modification to account for regions of sudden change in material properties. To this end, they introduced an effective length by correlating the beam deflections from both approaches. Ansari and Sahmani (2011b) used the Gurtin and Murdoch theory to investigate the bending and buckling of nanobeams with different boundary conditions. They derived explicit formulas for the Euler-Bernoulli, Timoshenko, Reddy and Levinson beam

* Corresponding author. Tel./fax: +98 131 6690276.
E-mail address: r_ansari@guilan.ac.ir (R. Ansari).

0997-7538/$ – see front matter © 2013 Elsevier Masson SAS. All rights reserved.
http://dx.doi.org/10.1016/j.euromechsol.2013.11.002

theories. Their study revealed that the bending and buckling responses of nanobeams are considerably affected by the surface stress effects. Gheshlaghi and Hasheminejad (2011) analyzed the nonlinear flexural vibrations of simply-supported Euler–Bernoulli nanobeams via an exact solution method with the consideration of surface stress effect. Using the Gurtin and Murdoch elasticity theory and Euler–Bernoulli beam theory, Nazemnezhad et al. (2012) studied the nonlinear free vibration of nanobeams under simply-supported boundary conditions. Their work indicated that the surface stress effect is independent of amplitude ratio. Ansari and his co-workers (Ansari et al., 2013) presented a numerical study on the vibrations of nanobeams accounting for surface stress effects. They employed the Gurtin and Murdoch theory to consider the surface effects and the formulation of the problem was based on the Euler-Bernoulli beam theory. They showed that the effect of surface stress is dependent on nanobeam's aspect ratio and thickness. Based on the Euler-Bernoulli beam theory, Asgharifard Sharabiani and Haeri Yazdi (2013) studied the nonlinear free vibration of functionally graded nanobeams subject to different boundary conditions with the consideration of surface effects.

In the present paper, the nonlinear free vibration of Timoshenko nanobeams with various boundary conditions is studied. To consider the surface stress effect, the Gurtin–Murdoch continuum elasticity is used. Derivation of the nonlinear governing equations and boundary conditions is based on Hamilton's principle and von Kármán geometric nonlinearity. To numerically solve the problem, first, the generalized differential quadrature (GDQ) method is used so as to discretize the governing equations and boundary conditions on space domain. In the next step, a Galerkin scheme is numerically applied for reducing the size of problem by using a small number of generalized variables. The resulting generalized governing equations on time domain are also discretized by a set of time periodic differential operators which are derived on the basis of the derivatives of a periodic base function. The pseudo arc-length continuation method is finally used to obtain the nonlinear frequency response of nanobeams.

2. Governing equations and boundary conditions

The schematic view of a nanobeam with length L and rectangular cross-section of thickness h shown in Fig. 1. A coordinate system x, y, z is used on the central axis of the beam, in which the x axis is taken along the length of the nanobeam, the y axis along the width direction and the z axis is taken along the height direction. The origin of the coordinate system is also chosen at the left end of the nanobeam. Based on the Timoshenko beam theory (Timoshenko, 1921, 1922), the displacement filed (u_x, u_y, u_z) is given by

$$u_x = u(t,x) - z\psi(t,x), \quad u_y = 0, \quad u_z = w(t,x) \tag{1}$$

where $u(t,x)$, $w(t,x)$, and $\psi(t,x)$ respectively represent the axial displacement of the center of cross section, transverse deflection, and the rotation angle of the cross section with respect to the vertical direction. Using the von Kármán hypothesis, the nonlinear strain–displacement relations can be written as

$$\varepsilon_{xx} = \frac{\partial u}{\partial x} - z\frac{\partial \psi}{\partial x} + \frac{1}{2}\left(\frac{\partial w}{\partial x}\right)^2, \quad \varepsilon_{xz} = \frac{1}{2}\left(\frac{\partial w}{\partial x} - \psi\right) \tag{2}$$

According to the linear elasticity, the stress components are expressed by

$$\sigma_{xx} = (\lambda + 2\mu)\left(\frac{\partial u}{\partial x} - z\frac{\partial \psi}{\partial x} + \frac{1}{2}\left(\frac{\partial w}{\partial x}\right)^2\right), \quad \sigma_{xz} = \mu k_s\left(\frac{\partial w}{\partial x} - \psi\right) \tag{3}$$

In Eq. (3) k_s is the shear correction factor. Also, λ and μ are the Lamé parameters which are defined as

$$\lambda = \frac{E\nu}{(1+\nu)(1-2\nu)}, \quad \mu = \frac{E}{2(1+\nu)} \tag{4}$$

where E and ν stand for Young's modulus and Poisson's ratio of the nanobeam, respectively.

To consider the size effects, the Gurtin–Murdoch theory (Gurtin and Murdoch, 1975, 1978) is used herein. Because of interaction between the elastic surface and bulk material, in-plane forces in different directions act on the nanobeam. The surface constitutive equations can be given as

$$\begin{aligned} \sigma^s_{\alpha\beta} &= \tau^s\delta_{\alpha\beta} + (\tau^s + \lambda^s)\varepsilon_{\gamma\gamma}\delta_{\alpha\beta} + 2(\mu^s - \tau^s)\varepsilon_{\alpha\beta} + \tau^s u^s_{\alpha,\beta} \\ \sigma^s_{\alpha z} &= \tau^s u^s_{z,\alpha}, \quad (\alpha, \beta = x, y) \end{aligned} \tag{5}$$

in which λ^s and μ^s show the surface Lamé parameters and τ^s is the residual surface stress under unstrained conditions. Also, $\delta_{\alpha\beta}$ denotes the Kronecker delta. Using Eq. (5), the surface stress components can be derived as

$$\begin{aligned} \sigma^s_{xx} &= (\lambda_s + 2\mu_s)\left(\frac{\partial u}{\partial x} + \frac{1}{2}\left(\frac{\partial w}{\partial x}\right)^2 - z\frac{\partial \psi}{\partial x}\right) - \frac{\tau_s}{2}\left(\frac{\partial w}{\partial x}\right)^2 + \tau_s, \\ \sigma^s_{xz} &= \tau_s\frac{\partial w}{\partial x} \end{aligned} \tag{6}$$

Since the stress component σ_{zz} is small as compared to σ_{xx} and σ_{xz}, it is neglected in the classical beam theories. By such assumption, the surface conditions cannot be satisfied. Thus, in order to satisfy the surface conditions of the Gurtin–Murdoch model, it is assumed that σ_{zz} varies linearly through the thickness of nanobeam and satisfies the balance conditions on the surfaces (Lu et al., 2006). Therefore, σ_{zz} is given as follows

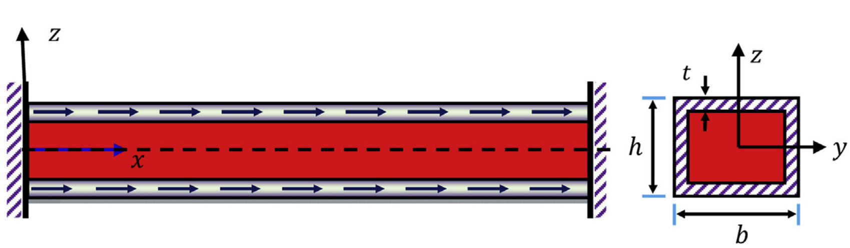

Fig. 1. Schematic view of a nanobeam with the selected coordinate system.

$$\sigma_{zz} = \frac{1}{2}\left\{\left(\frac{\partial\sigma_{xz}^{s+}}{\partial x} - \rho^{s+}\frac{\partial^2 w}{\partial t^2}\right) + \left(\frac{\partial\sigma_{xz}^{s-}}{\partial x} - \rho^{s-}\frac{\partial^2 w}{\partial t^2}\right)\right\} + \left\{\left(\frac{\partial\sigma_{xz}^{s+}}{\partial x} - \rho^{s+}\frac{\partial^2 w}{\partial t^2}\right) - \left(\frac{\partial\sigma_{xz}^{s-}}{\partial x} - \rho^{s-}\frac{\partial^2 w}{\partial t^2}\right)\right\}\frac{z}{h} \tag{7}$$

in which σ_{xz}^{s+} and σ_{xz}^{s-} are stresses at the top and bottom surfaces, respectively. Using Eq. (5), one can arrive at

$$\sigma_{zz} = \frac{2z}{h}\left(\tau_s\frac{\partial^2 w}{\partial x^2} - \rho_s\frac{\partial^2 w}{\partial t^2}\right) \tag{8}$$

where ρ_s is called surface mass density. By using σ_{zz} given in Eq. (8), the components of stress for the bulk of nanobeam can be modified as

$$\begin{aligned}
\sigma_{xx} &= (\lambda+2\mu)\left(\frac{\partial u}{\partial x} - z\frac{\partial\psi}{\partial x} + \frac{1}{2}\left(\frac{\partial w}{\partial x}\right)^2\right) + \frac{2\nu z}{(1-\nu)h}\left(\tau_s\frac{\partial^2 w}{\partial x^2} - \rho_s\frac{\partial^2 w}{\partial t^2}\right), \\
\sigma_{xz} &= \mu k_s\left(\frac{\partial w}{\partial x} - \psi\right)
\end{aligned} \tag{9}$$

The strain energy of nanobeam is written as

$$\begin{aligned}
\Pi_s &= \frac{1}{2}\iint \sigma_{ij}\varepsilon_{ij}\mathrm{d}A\mathrm{d}x + \frac{1}{2}\left(\int_{S^+}\sigma_{ij}^s\varepsilon_{ij}\mathrm{d}S^+ + \int_{S^-}\sigma_{ij}^s\varepsilon_{ij}\mathrm{d}S^-\right) \\
&= \frac{1}{2}\int_x\left\{\left(N_{xx}+\tilde{N}_{xx}\right)\left(\frac{\partial u}{\partial x} + \frac{1}{2}\left(\frac{\partial w}{\partial x}\right)^2\right) - \left(M_{xx}+\tilde{M}_{xx}\right)\frac{\partial\psi}{\partial x} + \left(Q+\tilde{Q}\right)\left(\frac{\partial w}{\partial x} - \psi\right)\right\}\mathrm{d}x
\end{aligned} \tag{10}$$

in which

$$\begin{aligned}
\tilde{N}_{xx} &= 2(b+h)(\lambda_s+2\mu_s)\left(\frac{\partial u}{\partial x} + \frac{1}{2}\left(\frac{\partial w}{\partial x}\right)^2\right) - (b+h)\tau_s\left(\frac{\partial w}{\partial x}\right)^2 + 2(b+h)\tau_s \\
\tilde{Q}_{xx} &= 2(b+h)\tau_s\frac{\partial w}{\partial x} \\
\tilde{M}_{xx} &= -(\lambda_s+2\mu_s)\left(\frac{bh^2}{2} + \frac{h^3}{6}\right)\frac{\partial\psi}{\partial x} \\
\cdot N_{xx} &= bh(\lambda+2\mu)\left(\frac{\partial u}{\partial x} + \frac{1}{2}\left(\frac{\partial w}{\partial x}\right)^2\right) \\
Q &= bh\mu k_s\left(\frac{\partial w}{\partial x} - \psi\right) \\
M_{xx} &= -\frac{bh^3(\lambda+2\mu)}{12}\frac{\partial\psi}{\partial x} + \frac{\nu bh^2\tau_s}{6(1-\nu)}\frac{\partial^2 w}{\partial x^2} - \frac{\nu bh^2\rho_s}{6(1-\nu)}\frac{\partial^2 w}{\partial t^2}
\end{aligned} \tag{11}$$

Moreover, the kinetic energy can be expressed as

$$\Pi_T = \frac{1}{2}\int_x\left\{(\rho bh + 2(b+h)\rho^s)\left[\left(\frac{\partial u}{\partial t}\right)^2 + \left(\frac{\partial w}{\partial t}\right)^2\right] + \left(\frac{\rho bh^3}{12} + \rho_s\left(\frac{bh^2}{2} + \frac{h^3}{6}\right)\right)\left(\frac{\partial\psi}{\partial t}\right)^2\right\}\mathrm{d}x \tag{12}$$

in which ρ is the bulk mass density. The work done by the axial force N_{0x} can be obtained by

$$\Pi_P = \frac{1}{2}\int_0^L N_{0x}\left(\frac{\partial w}{\partial x}\right)^2\mathrm{d}x \tag{13}$$

By employing the Hamilton principle

$$\delta\int_{t_1}^{t_2}(\Pi_T - \Pi_s + \Pi_P)\mathrm{d}t = 0 \tag{14}$$

the following equations of motion are derived

$$\frac{\partial\left(N_{xx}+\tilde{N}_{xx}\right)}{\partial x} = (\rho bh + 2(b+h)\rho^s)\frac{\partial^2 u}{\partial t^2}, \tag{15a}$$

$$\frac{\partial\left(Q+\tilde{Q}\right)}{\partial x} + \frac{\partial}{\partial x}\left(\left(N_{xx}+\tilde{N}_{xx}\right)\frac{\partial w}{\partial x}\right) - N_{0x}\frac{\partial^2 w}{\partial x^2} = (\rho bh + 2(b+h)\rho^s)\frac{\partial^2 w}{\partial t^2}, \tag{15b}$$

$$Q + \tilde{Q} - \frac{\partial\left(M_{xx}+\tilde{M}_{xx}\right)}{\partial x} = \frac{\rho bh^3}{12}\frac{\partial^2\psi}{\partial t^2} \tag{15c}$$

Furthermore, the associated boundary conditions are obtained as

$$\delta u = 0 \quad \text{or} \quad \delta\left(N_{xx}+\tilde{N}_{xx}\right) = 0, \tag{16a}$$

$$\delta w = 0 \quad \text{or} \quad \delta\left(\left(N_{xx}+\tilde{N}_{xx}\right)\frac{\partial w}{\partial x} + Q + \tilde{Q}\right) = 0, \tag{16b}$$

$$\delta\psi = 0 \quad \text{or} \quad \delta\left(M_{xx}+\tilde{M}_{xx}\right) = 0. \tag{16c}$$

Eq. (15) in terms of displacements are rewritten as

$$A_{11}\left(\frac{\partial^2 u}{\partial x^2} + \frac{\partial w}{\partial x}\frac{\partial^2 w}{\partial x^2}\right) - A_{33}\frac{\partial w}{\partial x}\frac{\partial^2 w}{\partial x^2} = I_1\frac{\partial^2 u}{\partial t^2}, \tag{17a}$$

$$\begin{aligned}
&A_{13}\left(\frac{\partial^2 w}{\partial x^2} - \frac{\partial\psi}{\partial x}\right) + A_{33}\frac{\partial^2 w}{\partial x^2} \\
&+ \left(A_{11}\frac{\partial u}{\partial x} + \frac{1}{2}(A_{11}-A_{33})\left(\frac{\partial w}{\partial x}\right)^2 + A_{33}\right)\frac{\partial^2 w}{\partial x^2} \\
&+ \left(A_{11}\frac{\partial^2 u}{\partial x^2} + (A_{11}-A_{33})\frac{\partial w}{\partial x}\frac{\partial^2 w}{\partial x^2}\right)\frac{\partial w}{\partial x} - N_{0x}\frac{\partial^2 w}{\partial x^2} = I_1\frac{\partial^2 w}{\partial t^2},
\end{aligned} \tag{17b}$$

$$A_{13}\left(\frac{\partial w}{\partial x} - \psi\right) + A_{33}\frac{\partial w}{\partial x} + D_{11}\frac{\partial^2\psi}{\partial x^2} - E_{11}\frac{\partial^3 w}{\partial x^3} = I_3\frac{\partial^2\psi}{\partial t^2} + G\frac{\partial^3 w}{\partial t^2\partial x} \tag{17c}$$

where

$$\begin{aligned}
&A_{11} = bh(\lambda+2\mu) + 2(b+h)(\lambda_s+2\mu_s), \quad A_{33} = 2(b+h)\tau_s, \\
&A_{13} = bh\mu k_s, \\
&D_{11} = (\lambda+2\mu)\frac{bh^3}{12} + (\lambda_s+2\mu_s)\left(\frac{bh^2}{2} + \frac{h^3}{6}\right), \quad E_{11} = \frac{\nu bh^2\tau_s}{6(1-\nu)} \\
&I_1 = \rho bh + 2(b+h)\rho^s, \quad I_3 = \frac{\rho bh^3}{12} + \rho_s\left(\frac{bh^2}{2} + \frac{h^3}{6}\right), \\
&G = -\frac{\nu bh^2\rho_s}{6(1-\nu)}
\end{aligned} \tag{18}$$

Also, the boundary conditions are

- Simply-supported boundary condition (SS)

$$u = w = M_{xx} + \tilde{M}_{xx} = 0 \ \ at \ \ ends \tag{19}$$

- Clamped boundary condition (C)

$$u = w = \psi = 0 \ \ at \ \ ends \tag{20}$$

3. Solution procedure

First, by introducing the following dimensionless parameters

$$u = LU, \quad w = hW, \quad X = \frac{x}{L}, \quad \xi = \frac{h}{L}, \quad \tau = \frac{t}{L}\sqrt{\frac{A_{110}}{I_{10}}} \tag{21}$$

the dimensionless form of Eq. (17) can be represented as follows

$$a_{11}\frac{\partial^2 U}{\partial X^2} + (a_{11} - a_{33})\xi^2\frac{\partial W}{\partial X}\frac{\partial^2 W}{\partial X^2} = I_1^*\frac{\partial^2 U}{\partial \tau^2} \tag{22a}$$

$$\begin{aligned}&(a_{13} + 3a_{33})\xi\frac{\partial^2 W}{\partial X^2} - a_{13}\frac{\partial \psi}{\partial X} + a_{11}\xi\left(\frac{\partial U}{\partial X}\frac{\partial^2 W}{\partial X^2} + \frac{\partial^2 U}{\partial X^2}\frac{\partial W}{\partial X}\right)\\ &+\frac{3}{2}(a_{11} - a_{33})\xi^3\frac{\partial^2 W}{\partial X^2}\left(\frac{\partial W}{\partial X}\right)^2 - \tilde{N}_x\xi\frac{\partial^2 W}{\partial X^2} = I_1^*\xi\frac{\partial^2 W}{\partial \tau^2}\end{aligned} \tag{22b}$$

$$\begin{aligned}&\frac{\partial^2 W}{\partial \tau^2}(a_{13} + a_{33})\xi\frac{\partial W}{\partial X} - a_{13}\psi + d_{11}\xi^2\frac{\partial^2 \psi}{\partial X^2} - e_{11}\xi^3\frac{\partial^3 W}{\partial X^3}\\ &= I_3^*\xi^2\frac{\partial^2 \psi}{\partial \tau^2} + g\xi^3\frac{\partial^3 W}{\partial \tau^2 \partial X}\end{aligned} \tag{22c}$$

$$\mathscr{D}_{ij}^r = \begin{cases} \mathbf{I}_x, & r = 0 \\ \dfrac{\mathscr{P}(x_i)}{(x_i - x_j)\mathscr{P}(x_j)}, & i \neq j \text{ and } i,j = 1,\ldots,N \text{ and } r = 1 \\ r\left[\mathscr{D}_{ij}^1\mathscr{D}_{ii}^{r-1} - \dfrac{\mathscr{D}_{ij}^{r-1}}{x_i - x_j}\right], & i \neq j \text{ and } i,j = 1,\ldots,N \text{ and } r = 2,3,\ldots N-1 \\ -\displaystyle\sum_{j=1;j\neq i}^{N}\mathscr{D}_{ij}^r, & i = j \text{ and } i,j = 1,\ldots,N \text{ and } r = 1,2,3,\ldots N-1 \end{cases} \tag{30}$$

where

$$\begin{aligned}&A_{110} = bh(\lambda + 2\mu), \ \ I_{10} = \rho h\\ &\{a_{11}, a_{13}, a_{33}\} = \{A_{11}, A_{13}, A_{33}\}/A_{110}, \quad d_{11} = \tfrac{D_{11}}{A_{110}h^2},\\ &e_{11} = \tfrac{E_{11}}{A_{110}h^2}\\ &I_1^* = \tfrac{I_1}{I_{10}}, \quad I_3^* = \tfrac{I_3}{I_{10}h^2}, \quad g = \tfrac{G}{I_{10}h^2}, \quad \omega = \Omega L\sqrt{I_{10}/A_{110}}\end{aligned} \tag{23}$$

Boundary conditions can also be expressed in dimensionless forms in a similar way;

- Simply-supported boundary condition:

$$U = W = e_{11}\xi\frac{\partial^2 W}{\partial X^2} - d_{11}\frac{\partial \psi}{\partial X} = 0 \tag{24}$$

- Clamped boundary condition:

$$U = W = \psi = 0 \tag{25}$$

3.1. GDQ Method

On the basis of the GDQ method (Shu, 2000) the rth derivative of $f(x)$ can be obtained as a linear sum of the function, i.e.

$$\left.\frac{\partial^r f(x)}{\partial x^r}\right|_{x=x_i} = \sum_{j=1}^{N}\mathscr{D}_{ij}^r f(x_j) \tag{26}$$

in which N is the number of total discrete grid points used in the process of approximation in the x direction and $\mathscr{D}_{ij}^r$ shows the weighting coefficients. A column vector F can be defined as

$$\mathbf{F} = [F_j] = [f(x_j)] = [f(x_1), f(x_2), \ldots, f(x_N)]^T \tag{27}$$

where $f(x_j)$ denotes the nodal value of $f(x)$ at $x = x_j$. A differential matrix operator based on Eq. (26) can be written in the form

$$\frac{\partial^r}{\partial x^r}(\mathbf{F}) = \mathbf{D}_x^r\mathbf{F} = [D_x^r]_{i,j}\{F_j\} \tag{28}$$

where

$$\mathbf{D}_x^r = [D_x^r]_{i,j} = \mathscr{D}_{ij}^r, \quad i,j = 1:N \tag{29}$$

In Eq. (29) r is the order of differentiation and $\mathscr{D}_{ij}^r$ is obtained by

in which $\mathscr{P}(x_i) = \prod_{j=1;\,j\neq i}^{N}(x_i - x_j)$, and $\mathbf{I}_x$ is a $N \times N$ identity matrix.

3.2. Discretization

One-dimensional functions $U(X)$,$W(X)$ and $\psi(X)$ are defined on$0 \leq X \leq 1$. Previous studies (e.g., (Tornabene and Viola, 2008)) revealed that the Chebyshev–Gauss–Lobatto grid point distribution has the most convergence and stability among the other grid distributions. Thus, using this grid distribution, the mesh can be generated as

$$X_i = \frac{1}{2}\left(1 - \cos\frac{i-1}{N-1}\pi\right), \quad i = 1:N \tag{31}$$

By introducing column vectors U,W and Ψ.

$$\mathbf{U^T} = [U_1, \ldots, U_N], \quad \mathbf{W^T} = [W_1, \ldots, W_N], \quad \mathbf{\Psi^T} = [\Psi_1, \ldots, \Psi_N] \tag{32}$$

in which $U_i = U(X_i), W_i = W(X_i), \Psi_i = \psi(X_i)$, Eq. (22) can be discretized as follows

$$\mathbf{M\ddot{X}} + \mathbf{KX} + \mathbf{R^{NL}}(X) = 0, \quad \mathbf{X}^T = \left[\mathbf{U_d^T}, \mathbf{w_d^T}, \mathbf{\Psi_d^T}\right] \tag{33}$$

where

$$\mathbf{M} = \begin{bmatrix} I_1^*\mathbf{D}_X^0 & 0 & 0 \\ 0 & I_1^*\mathbf{D}_X^0 & 0 \\ 0 & g\xi^3\mathbf{D}_X^1 & I_3^*\xi^2\mathbf{D}_X^0 \end{bmatrix}$$

$$\mathbf{K} = \begin{bmatrix} a_{11}\mathbf{D}_X^2 & 0 & 0 \\ 0 & (a_{13}+3a_{33})\xi\mathbf{D}_X^2 & -a_{13}\mathbf{D}_X^1 \\ 0 & (a_{13}+a_{33})\xi\mathbf{D}_X^1 - e_{11}\xi^3\mathbf{D}_X^3 & -a_{13}\mathbf{D}_X^0 + d_{11}\xi^2\mathbf{D}_X^2 \end{bmatrix},$$

$$\mathbf{R^{NL}}(\mathbf{X}) = \begin{bmatrix} \mathbf{R}_u \\ \mathbf{R}_w \\ 0 \end{bmatrix} \tag{34}$$

in which

$$\mathbf{R}_u = (a_{11} - a_{33})\xi^2\left(\mathbf{D}_X^2\mathbf{W}\right)\circ\left(\mathbf{D}_X^1\mathbf{W}\right)$$

$$\mathbf{R}_w = a_{11}\xi\left(\left(\mathbf{D}_X^2\mathbf{U}\right)\circ\left(\mathbf{D}_X^1\mathbf{W}\right) + \left(\mathbf{D}_X^2\mathbf{W}\right)\circ\left(\mathbf{D}_X^1\mathbf{U}\right)\right) + \frac{3}{2}(a_{11} - a_{33})\xi^3\left(\mathbf{D}_X^2\mathbf{W}\right)\circ\left(\mathbf{D}_X^1\mathbf{W}\right)\circ\left(\mathbf{D}_X^1\mathbf{W}\right) \tag{35}$$

In Eq. (35) $\circ$ denotes the Hadamard matrix product (see Appendix A). The boundary conditions (Eqs. (24) and (25)) can also be discretized in a similar procedure. By neglecting the nonlinear term, $\mathbf{R}^{NL}$, and by assuming harmonic solution $\mathbf{X} = \overline{\mathbf{X}}e^{i\omega t}$, one can arrive at

$$-\omega^2\mathbf{M}\overline{\mathbf{X}} + \mathbf{K}\overline{\mathbf{X}} = \left(\mathbf{K} - \omega^2\mathbf{M}\right)\overline{\mathbf{X}} = 0 \tag{36}$$

After substituting the boundary conditions into the stiffness and inertia matrices and then rearranging the governing equations and the boundary conditions within a standard eigenvalue problem, it is possible to obtain

$$\begin{bmatrix} \mathbf{K}_{dd} & \mathbf{K}_{db} \\ \mathbf{K}_{bd} & \mathbf{K}_{bb} \end{bmatrix}\begin{bmatrix} \overline{\mathbf{X}}_d \\ \overline{\mathbf{X}}_b \end{bmatrix} = \begin{bmatrix} \omega^2\mathbf{M}_{dd}\overline{\mathbf{X}}_d \\ 0 \end{bmatrix} \tag{37}$$

where subscripts b and d denote the boundary and domain grid points, respectively. Eq. (37) can be uncoupled as the following form

$$\begin{cases} \left(K_{dd} - K_{db}(K_{bb})^{-1}K_{bd}\right)\overline{X}_{\boldsymbol{d}} = \omega^2 M_{dd}\overline{X}_{\boldsymbol{d}} \\ \overline{X}_b = (K_{bb})^{-1}K_{bd}\overline{X}_{\boldsymbol{d}} \end{cases} \tag{38}$$

By solving the set of linear equations of Eq. (38), the natural frequencies ω and their associated vibration mode shapes are obtained.

3.3. Reduction of the number of space-domain variables

Here, a Galerkin-based method is numerically applied so as to reduce the set of nonlinear equations of Chan and Hsiao (1985) into a Duffing-type set of ordinary differential equations. In this regard, one can reduce the size of problem by using of a small number of generalized variables $\mathbf{q}$ (Chan and Hsiao, 1985). For this purpose, the large number of displacement freedoms $\mathbf{X}$ can be represented in the form of following transformation

$$X = \Phi q \tag{39}$$

where $\mathbf{\Phi}$ is a sparse matrix assembled by basis vectors which contains the first m eigenvectos. It should be mentioned that as the first few eigenvectors dominate the preliminary stages of the nonlinear behavior of structure and in addition satisfy both types of boundary conditions (i.e. essential and natural), they can be regarded as suitable candidates for the reduced analysis (Chan and Hsiao, 1985). The reduced generalized coordinates vector and transformation matrix $\mathbf{\Phi}$ are written as

$$q^T_{(3m)\times 1} = \left[q_u^1, q_u^2, \ldots, q_u^m, q_w^1, q_w^2, \ldots, q_w^m, q_\psi^1, q_\psi^2, \ldots, q_\psi^m\right] \tag{40}$$

$$\mathbf{\Phi}_{(3N)\times(2m)} = \begin{bmatrix} \mathbf{\Phi}_{\boldsymbol{u}} & & \\ & \mathbf{\Phi}_{\boldsymbol{w}} & \\ & & \mathbf{\Phi}_\psi \end{bmatrix}$$

$$\mathbf{\Phi}_{\boldsymbol{u}_{N\times m}} = \left[\{\overline{X}_{\mathrm{u}}^1\}_{N\times 1}, \ldots, \{\overline{X}_{\mathrm{u}}^m\}_{N\times 1}\right] \tag{41}$$

$$\mathbf{\Phi}_{\boldsymbol{w}_{N\times m}} = \left[\{\overline{X}_{\mathrm{w}}^1\}_{N\times 1}, \ldots, \{\overline{X}_{\mathrm{w}}^m\}_{N\times 1}\right]$$

$$\mathbf{\Phi}_{\psi_{N\times m}} = \left[\{\overline{X}_\psi^1\}_{N\times 1}, \ldots, \{\overline{X}_\psi^m\}_{N\times 1}\right]$$

Substituting Eq. (39) into (33) gives the residual as

$$\mathbf{R} = \mathbf{M\Phi\ddot{q}} + \mathbf{K\Phi}\mathrm{q} + \mathbf{R^{NL}}(\mathbf{\Phi}\mathrm{q}) \tag{42}$$

In the present numerical Galerkin method, multiplying each equation by associated eigenvectors and integrating over the domain can be simultaneously done using the following matrix operator

$$\mathbf{G}_{m\times 3N} = \left(\mathbf{S}\diamond\mathbf{\Phi}^{\mathrm{T}}\right), \quad \mathbf{S} = \{\mathbf{S}_X, \mathbf{S}_X, \mathbf{S}_X\}_{1\times(3N)} \tag{43}$$

in which $\mathbf{S}_X$ is an integral operator (see Appendix B). Through multiplying Eq. (43) by the residual vector (Eq. (42)), the reduced form of Eq. (33) can be expressed by

$$\tilde{\mathbf{M}}\ddot{\mathbf{q}} + \tilde{\mathbf{K}}\mathbf{q} + \tilde{\mathbf{R}}^{NL}(\mathbf{q}) = 0 \tag{44}$$

which is a set of nonlinear ordinary differential equations. Moreover

$$\tilde{\mathbf{M}} = \mathbf{GM\Phi}, \quad \tilde{\mathbf{K}} = \mathbf{GK\Phi}, \quad \tilde{\mathbf{N}}(\mathbf{q}) = \mathbf{GR^{NL}}(\mathbf{\Phi}\mathrm{q}). \tag{45}$$

It is seen that the general coordinates are reduced from $3N$ discrete points to $3m$ ones, where N and m respectively show the number of discrete points in the GDQ method and the number of selected mode shapes in the Galerkin method and $1 \le m \le N$. Also, it should be noted that both essential and natural boundary conditions are satisfied in the present approach since the linear mode shapes used in the Galerkin method are obtained from a numerical procedure. Additionally, it should be remarked that the surface stress effects are incorporated into the analysis as the linear mode shapes employed in the solution method are obtained from the surface elasticity theory. Thus, one can conclude that with the present numerical Galerkin method the desired accuracy can be achieved using a small number of mode shapes and therefore the computational effort considerably is reduced.

3.4. Time-Domain solution

By defining $t = \tau/T$, Eq. (44) can be rewritten as

$$\frac{1}{T^2}\tilde{\mathbf{M}}\ddot{\mathbf{q}} + \tilde{\mathbf{K}}\mathbf{q} + \tilde{\mathbf{R}}^{NL}(\mathbf{q}) = 0 \tag{46}$$

For a periodic motion, the following conditions must be satisfied

$$\begin{cases} \mathbf{q}|_{\tau=0} = \mathbf{q}|_{\tau=1} \\ \left.\frac{d\mathbf{q}}{d\tau}\right|_{\tau=0} = \left.\frac{d\mathbf{q}}{d\tau}\right|_{\tau=1} \end{cases} \tag{47}$$

To find out the periodic response of nanobeam in the time period T, the general governing equation is discretized over the time domain via time differential matrix operators. The main idea for the solution of Eq. (46) under the periodic conditions of Eq. (47) is to select a specific grid and differential matrix operator for time domain which naturally satisfy the periodic conditions rather than imposing the periodic conditions on time domain differential operators. To accomplish this aim, an unbounded grid with periodic grid points between 0 and 1 is utilized in which only functions with fix periodicity are authorized. Also, spectral differentiation matrix operators are obtained from derivatives of periodic sinc function, $\sin(\pi t/h)/((2\pi/h)\tan(t/2))$, as a base function in a collocation method where $h = 2\pi/n$ (Trefethen, 2000). The periodic grid points are given by

$$\tau_i = \frac{i}{n}, \quad 0 < \tau_i \le 1, \quad i = 1, 2, \ldots, k. \tag{48}$$

where k shows the number of discrete points in the time domain. By extending the field vector in time as $\mathbf{Q}_{m\times k} = [\mathbf{q}^1_{m\times 1}, \mathbf{q}^2_{m\times 1}, \ldots, \mathbf{q}^k_{m\times 1}]$, the general governing equations are discretized in the following forms

$$\frac{1}{T^2}\tilde{\mathbf{M}}\ddot{\mathbf{Q}} + \tilde{\mathbf{K}}\mathbf{Q} + \tilde{\mathbf{R}}^{NL}(\mathbf{Q}) = 0, \tag{49a}$$

$$\frac{1}{T^2}\tilde{\mathbf{M}}\mathbf{Q}\tilde{\mathbf{D}}_{\mathbf{t}}^{(2)^{\mathrm{T}}} + \tilde{\mathbf{K}}\mathbf{Q} + \tilde{\mathbf{R}}_{\mathbf{nl}}(\mathbf{Q}) = 0 \tag{49b}$$

in which $\tilde{\mathbf{D}}_{\mathbf{t}}^{(2)}$ and $\tilde{\mathbf{D}}_{\mathbf{t}}^{(1)}$ are differential matrix operators for second and first time derivatives, respectively. Consider the relation $(\mathbf{B}^{\mathrm{T}} \otimes \mathbf{A})vec(\mathbf{X}) = vec(\mathbf{AXB})$ in which $\mathbf{A}$ and $\mathbf{B}$ are constant matrices, and $\mathbf{X}$ is an unknown matrix. Also, $vec(\mathbf{X})$ stands for the vectorization of the matrix $\mathbf{X}$ and $\otimes$. notes the Kronecker product (see Appendix A). Using this relation, the vectorized form of Eq. (49) can be expressed as

$$\frac{1}{T^2} vec\left(\tilde{\mathbf{M}}\mathbf{Q}\tilde{\mathbf{D}}_t^{(2)^{\mathrm{T}}}\right) + vec\left(\tilde{\mathbf{K}}\mathbf{Q}\mathbf{I}_t\right) + vec\left(\tilde{\mathbf{R}}_{\mathbf{nl}}(\mathbf{Q})\right) = 0 \tag{50a}$$

$$\left(\frac{1}{T^2}\tilde{\mathbf{D}}_\tau^{(2)} \otimes \tilde{\mathbf{M}} + \mathbf{I_t} \otimes \tilde{\mathbf{K}}\right) vec(\mathbf{Q}_\tau) + \overline{\mathbf{R}}_{\mathbf{nl}}(vec(\mathbf{Q}_\tau)) = 0 \tag{50b}$$

The explicit formulation for the first and second differential matrix operators $\tilde{\mathbf{D}}_\tau^{(1)}$ and $\tilde{\mathbf{D}}_\tau^{(2)}$ are given as

$$\begin{cases} a_{11} = 0 \\ a_{i,1} = \frac{(-1)^{i-1}}{2}\cot\frac{\pi(i-1)}{N_t} \\ a_{1,j} = \frac{(-1)^{N_t-j+1}}{2}\cot\frac{\pi(N_t-j+1)}{N_t} \\ a_{i+1,j+1} = a_{i,j} \end{cases}, \quad i,j = 2,3,4,\ldots,N_t, \quad \mathbf{D}_\tau^{(1)} = 2\pi[a_{i,j}] \tag{51a}$$

$$\begin{cases} b_{11} = -\frac{N_t^2}{12} - \frac{1}{6} \\ b_{i,1} = \frac{(-1)^{i-2}}{2\sin^2\frac{\pi(i-1)}{N_t}} \\ b_{1,j} = \frac{(-1)^{N_t-j}}{2\sin^2\frac{\pi(N_t-j+1)}{N_t}} \\ b_{i+1,j+1} = b_{i,j} \end{cases}, \quad i,j = 2,3,4,\ldots,N_t, \quad \mathbf{D}_\tau^{(2)} = (2\pi)^2[b_{i,j}] \tag{51b}$$

Note that $\tilde{\mathbf{D}}_\tau^{(1)}$ and $\tilde{\mathbf{D}}_\tau^{(2)}$ are Teoplitz matrices. After substituting Eq. (51) into (50b), the set of nonlinear equations of the domain can be shown as

$$\mathbf{H} : \mathbb{R}^{m\times k} + \mathbb{R}^1 \to \mathbb{R}^{m\times k}, \mathbf{H}(\mathrm{T}, \mathrm{vec}(\mathbf{Q}_{m\times k})) = 0 \tag{52}$$

Finally, by treating the period T, as a parameter, Eq. (52) is solved using the pseudo arc-length method (Keller, 1977) and Ω_{NL} is readily obtained from $2\pi/T$.

4. Results and discussion

In this section, numerical results are presented for the nonlinear vibration behavior of nanobeams with simply supported–simply supported (SS–SS), clamped–clamped (C–C) and simply supported-clamped (SS–C) boundary conditions. It is assumed that the material of nanobeams is silicon (Si) with the following bulk and surface properties (Miller and Shenoy, 2000; Zhu et al., 2006)

$$E = 210\ \mathrm{GPa}, \quad \rho = 2331\ \mathrm{kg/m^3}, \quad \nu = 0.24,$$
$$\lambda_s = -4.488\ \mathrm{N/m}, \quad \mu_s = -2.774\ \mathrm{N/m}, \quad \tau_s = 0.605\ \mathrm{N/m},$$
$$\rho_s = 3.17 \times 10^{-7}\ \mathrm{kg/m^2}$$

The dimensionless fundamental frequencies ω_L as a function of nanobeam's thickness predicted by the surface stress model are given in Table 1. The results of the classical model are also presented in this table. It is seen that with increasing the thickness of nanobeam, the frequency decreases and tends to that of classical model for large magnitudes of thickness. Moreover, Fig. 2 is given to highlight the difference between the results obtained based on the surface stress model and the ones obtained by its classical counterpart at different thicknesses. In this figure it is assumed that the length-to-thickness ratio, $\eta = L/h$, is equal to 10. It is observed that

Table 1
Dimensionless fundamental frequency ω_L of nanobeams with various thicknesses.

Thick. (nm)	C–C	SS–C	SS–SS
1	0.2524	0.2148	0.1830
2	0.2323	0.1904	0.1557
5	0.2117	0.1643	0.1255
50	0.1928	0.1388	0.0937
Classic	0.1902	0.1351	0.0887

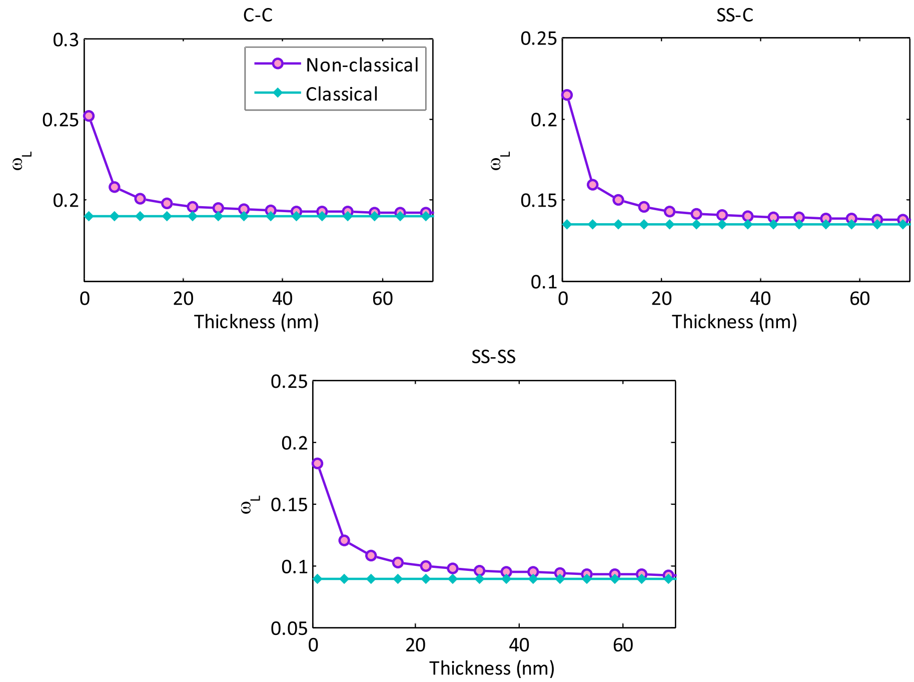

Fig. 2. Comparison between classical and non-classical beam models in predicting the nonlinear vibration behavior of nanobeams ($\eta = 10$).

the classical model tends to underestimate the frequency of nanobeam especially for small thicknesses. However, as the thickness of nanobeam increases, the surface stress effect diminishes so that the results of both models tend to converge.

Presented in Figs. 3–7 are the frequency–amplitude curves of nanobeams with different geometrical and surface properties. Fig. 3 shows the effect of thickness variation on the nonlinear free vibration behavior of nanobeams. As can be seen, with the increase of nanobeam's thickness, the normalized frequency increases especially for large magnitudes of dimensionless deflection, and in the limit the results of classical theory are obtained. Also, it is found that the effect of thickness is dependent on the type of boundary conditions. Fig. 4 is given to highlight the nonlinear free vibration characteristics of the nanobeams at short lengths using the Timoshenko beam theory which cannot be predicted by the Euler–Bernoulli beam theory. Illustrated in this figure are the frequency–amplitude curves for various length-to-thickness ratios, and it is seen that the normalized frequency becomes larger when η decreases. Figs. 5–7 show the effects of surface properties, i.e., $\lambda_s + 2\mu_s$, τ_s and ρ_s on the nonlinear vibration behavior. From Figs. 5

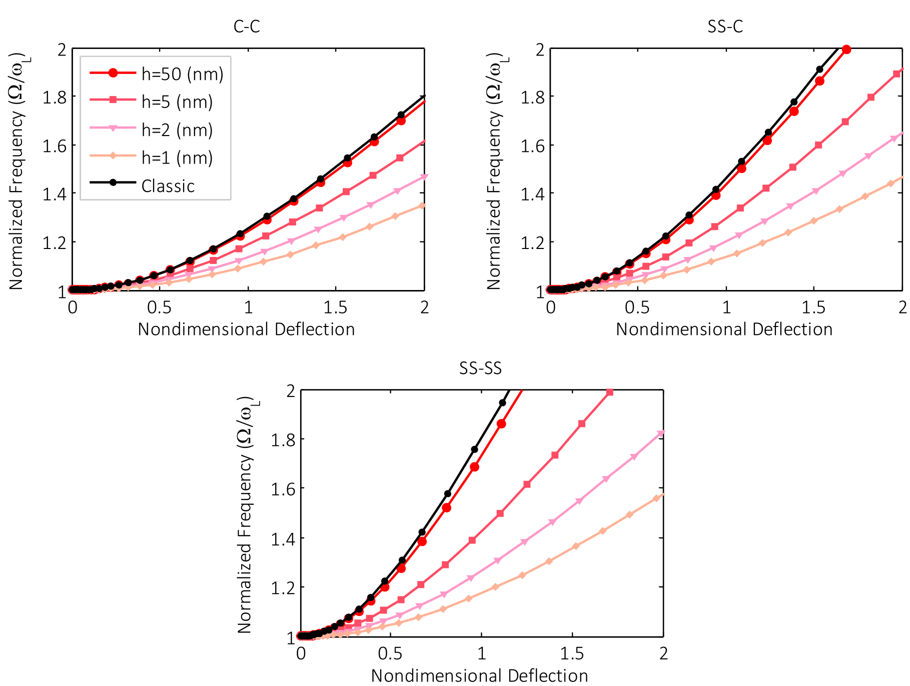

Fig. 3. Variation of normalized frequency versus dimensionless deflection for nanobeams with different thicknesses ($\eta = 10$).

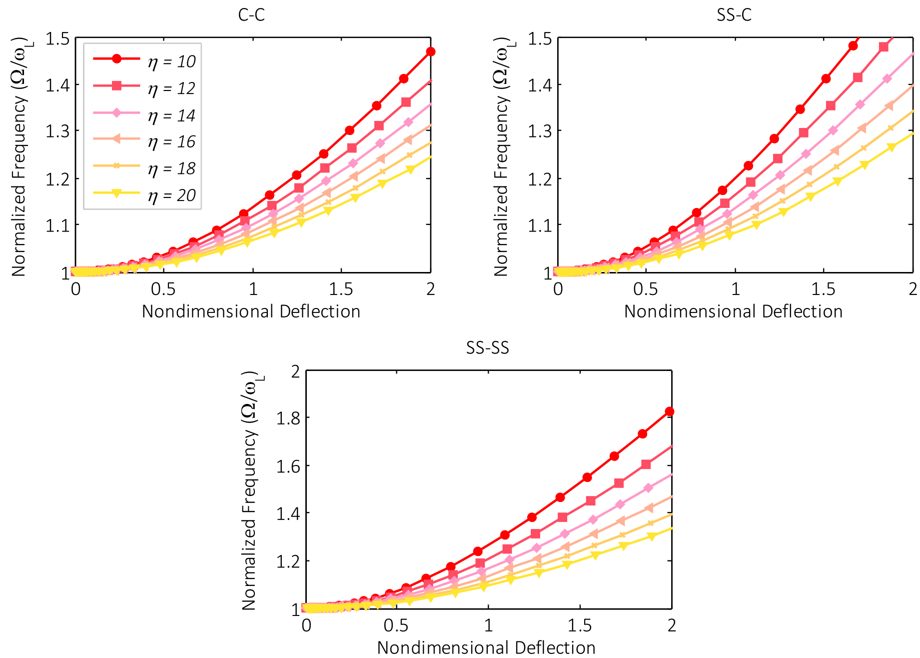

Fig. 4. Variation of normalized frequency versus dimensionless deflection for nanobeams with different length-to-thickness ratios ($h = 2\ nm$).

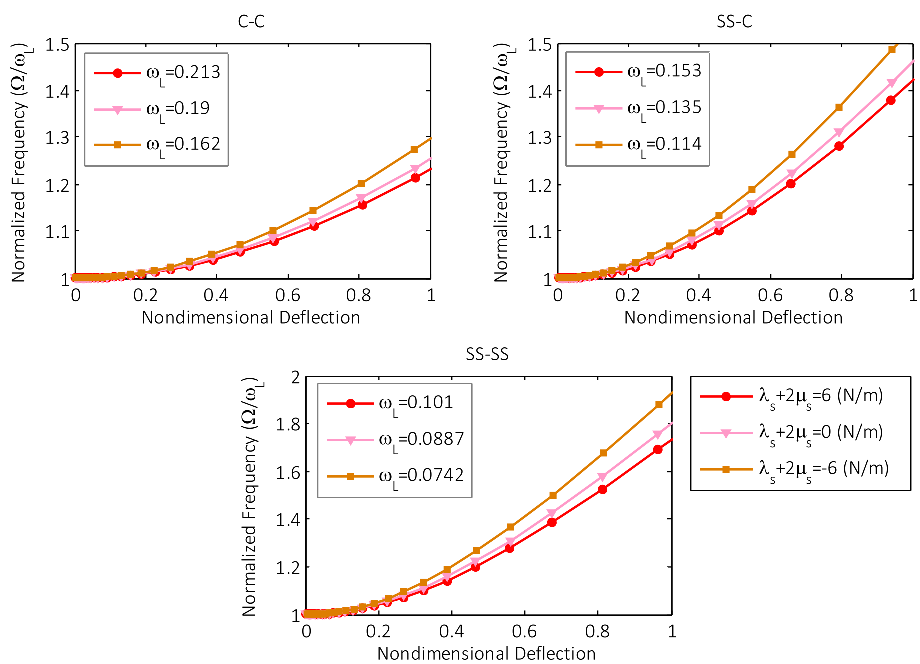

Fig. 5. Variation of normalized frequency versus dimensionless deflection for nanobeams with different values of $\lambda^s + 2\mu^s$ ($\tau^s = \rho^s = 0$, $h = 2\ \ nm$).

and 6, it can be observed that the normalized frequency decreases as $\lambda_s + 2\mu_s$ and τ_s increase. In addition, according to Fig. 7 one can find that the dimensionless fundamental frequency increases with the increase of ρ_s.

5. Conclusion

In this work, the free vibration analysis of nanobeams was presented in the nonlinear regime using the surface stress elasticity and Timoshenko beam theory. Hamilton's principle was used to obtain the nonlinear equations of motion and associated boundary conditions which were then discretized by the GDQ technique. The space-domain variables were reduced by a pseudo-Galerkin method and the set of partial differential governing equations were converted to a set of ordinary differential equations of Duffing-type. For the solution in the time-domain, after discretization via periodic time differential operators, the pseudo arc-length method was utilized to solve the resulting nonlinear algebraic parameterized equations. The numerical results showed that the surface stress effect is more important for thin nanobeams and the difference between the results of classical and non-classical model decreases as the thickness of nanobeam increases. Also,

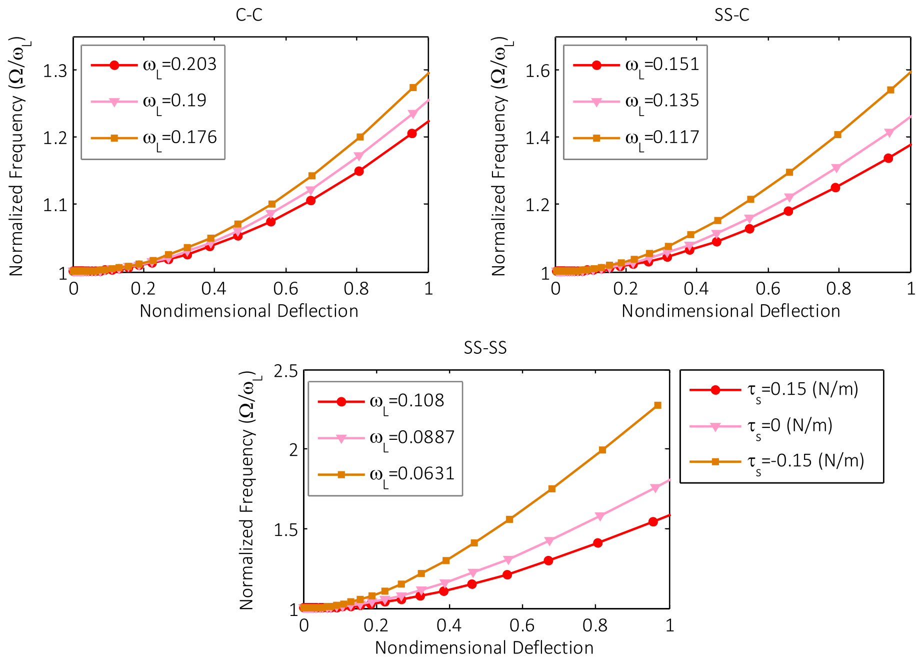

Fig. 6. Variation of normalized frequency versus dimensionless deflection for nanobeams with different values of τ^s ($2\mu^s + \lambda^s = \rho^s = 0$, $h = 2$ nm).

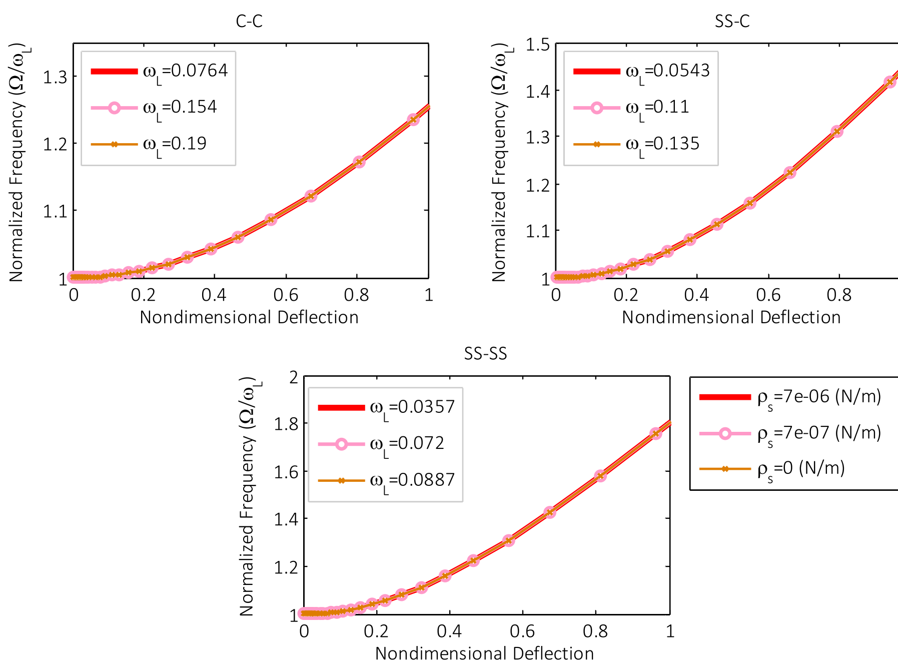

Fig. 7. Variation of normalized frequency versus dimensionless deflection for nanobeams with different values of ρ^s ($2\mu^s + \lambda^s = \tau^s = 0$, $h = 2$ nm).

the effects of surface properties on the nonlinear vibration behavior were examined and it was revealed that increasing the residual surface stress leads to increasing the dimensionless fundamental frequency while it decreases as the surface density becomes larger.

Appendix A. Hadamard and Kronecker Products

Definition 1. *Let* $\mathbf{A} = [A_{ij}]_{N\times M}$ *and* $\mathbf{B} = [B_{ij}]_{N\times M}$, *then the Hadamard product of these matrices take the form as* $\mathbf{A}\circ\mathbf{B} = [A_{ij}B_{ij}]_{N\times M}$.

Definition 2. *Let* $\mathbf{A}$ *be a m-by-n matrix and* $\mathbf{B}$ *a p-by-q matrix, then* $\mathbf{A}\otimes\mathbf{B} = \begin{bmatrix} a_{11}\mathbf{B} & \cdots & a_{1n}\mathbf{B} \\ \vdots & \ddots & \vdots \\ a_{m1}\mathbf{B} & \cdots & a_{mn}\mathbf{B} \end{bmatrix}_{mp\times nq}$ *indicates the Kronecker product of matrices* $\mathbf{A}$ *and* $\mathbf{B}$ *which is a mp-by-nq block matrix.*

Appendix B. Integral Operator

The *trapezoidal* rule can be employed as an integral matrix operator in the following form

$$\int_a^b f(x)\mathrm{d}x \approx \frac{1}{2}\mathbf{XWF} = \mathbf{S_x F}, \quad \mathbf{X} = \{x_1, x_2, \ldots, x_N\},$$
$$\mathbf{S_x} = \{S_x\}_{1\times N}$$

where $\boldsymbol{S_x}$ denotes the integral operator and $\mathbf{W}$ is an $N \times N$ matrix with the non-zero elements of

$$W_{i,j} = \begin{cases} 1, i-j = 1 \text{ or } i = j = N \\ -1, \ i-j = -1 \text{ or } i = j = 1 \end{cases}$$

References

Ansari, R., Sahmani, S., 2011. Surface stress effects on the free vibration behavior of nanoplates. Int. J. Eng. Sci. 49, 1204–1215.

Ansari, R., Sahmani, S., 2011. Bending behavior and buckling of nanobeams including surface stress effects corresponding to different beam theories. Int. J. Eng. Sci. 49, 1244–1255.

Ansari, R., Hosseini, K., Darvizeh, A., Daneshian, B., 2013. A sixth-order compact finite difference method for non-classical vibration analysis of nanobeams including surface stress effects. Appl. Math. Comput. 219, 4977–4991.

Asgharifard Sharabiani, P., Haeri Yazdi, M.R., 2013. Nonlinear free vibrations of functionally graded nanobeams with surface effects. Compos. Part B 45, 581–586.

Assadi, A., 2012. Size dependent forced vibration of nanoplates with consideration of surface effects. Appl. Math. Model 37, 3575–3588.

Bar On, B., Altus, E., Tadmor, E.B., 2010. Surface effects in non-uniform nanobeams: continuum vs. Atomistic modeling. Int. J. Solids Struct. 47, 1243–1252.

Chan, A.S.L., Hsiao, K.M., 1985. Nonlinear analysis using a reduced number of variables. Comput. Meth. Appl. Mech. Eng. 52, 899–913.

Daulton, T.L., Bondi, K.S., Kelton, K.F., 2010. Nanobeam diffraction fluctuation electron microscopy technique for structural characterization of disordered materials-application to $Al_{88-x}Y_7Fe_5Ti_x$ metallic glasses. Ultramicroscopy 110, 1279–1289.

Dingreville, R., Qu, J., Cherkaoui, M., 2005. Surface free energy and its effects on the elastic behavior of nano-sized particles, wires and films. J. Mech. Phys. Solids 53, 1827–1954.

Elishakoff, I., Pentaras, D., Dujat, K., Versaci, C., Muscolino, G., Storch, J., Bucas, S., Challamel, N., Natsuki, T., Zhang, Y.Y., Wang, C.M., Ghyselinck, G., 2012. Carbon Nanotubes and Nanosensors: Vibrations, Buckling and Ballistic Impact. Wiley–ISTE, London.

Fu, Y., Zhang, J., Jiang, Y., 2010. Influences of the surface energies on the nonlinear static and dynamic behaviors of nanobeams. Physica E 42, 2268–2273.

Gheshlaghi, B., Hasheminejad, S.M., 2011. Surface effects on nonlinear free vibration of nanobeams. Compos. Part B 42, 934–937.

Gurtin, M.E., Murdoch, A.I., 1975. A continuum theory of elastic material surface. Arch. Rat. Mech. Anal. 57, 291–323.

Gurtin, M.E., Murdoch, A.I., 1978. Surface stress in solids. Int. J. Solids Struct 14, 431–440.

Hu, B., Ding, Y., Chen, W., Kulkarni, D., Shen, Y., Tsukruk, V.V., Wang, Z.L., 2010. External-strain induced insulating phase transition in VO_2 nanobeam and its application as flexible strain sensor. Adv. Mater. 22, 5134–5139.

Keller, H.B., 1977. Numerical solution of bifurcation and nonlinear eigenvalue problems, applications of bifurcation theory. In: Proc. Advanced Sem., Univ. Wisconsin, Madison, Wis., 1976. Academic Press, New York, pp. 359–384.

Kirkby, K.J., Grime, G.W., Webb, R.P., Kirkby, N.F., Folkard, M., Prise, K., Vojnovic, B., 2007. A scanning focussed vertical ion nanobeam: a new UK Facility for Cell Irradiation and Analysis. Nucl. Instrum. Meth. Phys. Res. B 260, 97–100.

Li, Z.R., Lim, C.W., He, L.H., 2006. Stress concentration around a nano-scale spherical cavity in elastic media: effect of surface stress. Eur. J. Mech. A/Solids 25, 260–270.

Liu, J.L., Mei, Y., Xia, R., Zhu, W.L., 2012. Large displacement of a static bending nanowire with surface effects. Physica E 44, 2050–2055.

Lu, P., He, L.H., Lee, H.P., Lu, C., 2006. Thin plate theory including surface effects. Int. J. Solids Struct. 43, 4631–4647.

Maksymov, I.S., 2011. Optical switching and logic gates with hybrid plasmonic-photonic crystal nanobeam cavities. Phys. Lett. A 375, 918–921.

Miller, R.E., Shenoy, V.B., 2000. Size-dependent elastic properties of nanosized structural elements. Nanotechnology 11, 139–147.

Miri, A.K., Avazmohammadi, R., Yang, F., 2011. Effect of surface stress on the deformation of an elastic half-plane containing a nano-cylindrical hole under a surface loading. J. Comput. Theor. Nanosci. 8, 231–236.

Narendar, S., Gopalakrishnan, S., 2012. Study of Terahertz wave propagation properties in nanoplates with surface and small-scale effects. Int. J. Mech. Sci. 64, 221–231.

Narendar, S., Ravinder, S., Gopalakrishnan, S., 2012. Study of non-local wave properties of nanotubes with surface effects. Comput. Mater. Sci. 56, 179–184.

Nazemnezhad, R., Salimi, M., Hosseini Hashemi, Sh., Asgharifard Sharabiani, P., 2012. An analytical study on the nonlinear free vibration of nanoscale beams incorporating surface density effects. Compos. Part B 43, 2893–2897.

Nilsson, S.G., Sarwe, E.L., Montelius, L., 2003. Fabrication and mechanical characterization of ultrashort nanocantilevers. Appl. Phys. Lett. 83, 990–993.

Nilsson, S.G., Borrise, X., Montelius, L., 2004. Size effect on Young's modulus of thin chromium cantilevers. Appl. Phys. Lett. 85, 3555–3557.

Sadeghian, H., Goosen, J.F.L., Bossche, A., Thijsse, B.J., van Keulen, F., 2011. Effects of size and surface on the elasticity of silicon nanoplates: molecular dynamics and semi-continuum approaches. Thin Solid Films 520, 391–399.

Shambat, G., Ellis, B., Petykiewicz, J., Mayer, M.A., Sarmiento, T., Harris, J., Haller, E.E., Vuckovic, J., 2011. Nanobeam photonic crystal cavity light-emitting diodes. Appl. Phys. Lett. 99, 071105.

Shu, C., 2000. Differential Quadrature and its Application in Engineering. Springer, London.

Timoshenko, S.P., 1921. On the correction factor for shear of the differential equation for transverse vibrations of bars of uniform cross-section. Philos. Mag 41, 744–746.

Timoshenko, S.P., 1922. On the transverse vibrations of bars of uniform cross-section. Philos. Mag. 43, 125–131.

Tornabene, F., Viola, E., 2008. 2-D solution for free vibrations of parabolic shells using generalized differential quadrature method. Eur. J. Mech. – A/Solids 27, 1001–1025.

Trefethen, L.N., 2000. Spectral Methods in MATLAB. Oxford University, Oxford, England.

Wang, Z.Q., Zhao, Y.P., Huang, Z.P., 2010. The effects of surface tension on the elastic properties of nano structures. Int. J. Eng. Sci. 48, 140–150.

Zhu, R., Pan, E., Chung, P.W., Cai, X., Liew, K.M., Buldum, A., 2006. Atomistic calculation of elastic moduli in strained silicon. Semicond. Sci. Technol. 21, 906–911.